

11.0%


Date: 2023-06-14 20:26 UTC

* All sources 43 | Internet sources 41

- ✓ [3] pdfs.semanticscholar.org/55dd/10e1b932df6caf0282b1edae276a6b7211f1.pdf
5.3% 21 matches
- ✓ [4] www.jneurosci.org/content/18/10/3597
0.6% 8 matches
- ✓ [5] link.springer.com/article/10.1007/s11010-013-1835-z
0.8% 7 matches
- ✓ [6] mdpi-res.com/d_attachment/fermentation/fermentation-08-00634/article_deploy/fermentation-08-00634-s001.zip?version=1668249503
0.5% 7 matches
- ✓ [7] www.mdpi.com/1999-4923/15/4/1210/htm
0.4% 5 matches
- ✓ [8] www.sciencedirect.com/science/article/abs/pii/S0009279719312001
0.6% 4 matches
- ✓ [9] www.ncbi.nlm.nih.gov/pmc/articles/PMC6358285/
0.5% 4 matches
- ✓ [10] www.sciencedirect.com/science/article/abs/pii/S0925346718302258
0.6% 4 matches
- ✓ [11] www.sciencedirect.com/science/article/pii/S0021979719307118#:~:text=Magnetically separable catalysts attract considerable,noble metal nanoparticl
0.4% 4 matches
- ✓ [12] pubs.rsc.org/en/content/getauthorversionpdf/C5RA13837J
0.2% 5 matches
- ✓ [13] www.researchgate.net/publication/5387383_Zinc_Ferrite_Nanoparticles_as_MRI_Contrast_Agents
0.5% 1 matches
- ✓ [14] www.ncbi.nlm.nih.gov/pmc/articles/PMC7028487/
0.3% 3 matches
- ✓ [15] www.sciencedirect.com/science/article/abs/pii/089158499290176H
0.3% 4 matches
- ✓ [16] www.ncbi.nlm.nih.gov/pmc/articles/PMC5242349/
0.2% 3 matches
- ✓ [17] www.researchgate.net/figure/Dynamic-control-example-magnetic-particles-are-manipulated-to-the-centre-Reprinted-with_fig1_320631051
0.3% 1 matches
- ✓ [18] www.ncbi.nlm.nih.gov/pmc/articles/PMC8395693/
0.2% 3 matches
- ✓ [19] www.sciencedirect.com/science/article/pii/S2211812814006257
0.2% 2 matches
- ✓ [20] www.ncbi.nlm.nih.gov/pmc/articles/PMC7286314/
0.2% 2 matches
- ✓ [21] www.sciencedirect.com/science/article/abs/pii/S0254058422013037
0.2% 3 matches
- ✓ [22] www.ncbi.nlm.nih.gov/pmc/articles/PMC3126729/
0.1% 1 matches
- ✓ [23] www.sciencedirect.com/science/article/abs/pii/S0040609014009420
0.2% 2 matches
- ✓ [24] www.ncbi.nlm.nih.gov/pmc/articles/PMC28405/
0.1% 2 matches
- ✓ [25] infinitylearn.com/surge/blog/neet/cell-organelles-structure/
0.1% 2 matches
- ✓ [26] www.ncbi.nlm.nih.gov/pmc/articles/PMC7193251/
0.1% 2 matches
- ✓ [27] www.ncbi.nlm.nih.gov/pmc/articles/PMC2674643/
0.1% 2 matches

<input checked="" type="checkbox"/> [28]	www.sciencedirect.com/science/article/abs/pii/S0926337302001236 0.1% 2 matches
<input checked="" type="checkbox"/> [29]	www.sciencedirect.com/science/article/pii/S2238785420312503 0.1% 1 matches
<input checked="" type="checkbox"/> [30]	www.sciencedirect.com/science/article/pii/S004040201401000X 0.1% 1 matches
<input checked="" type="checkbox"/> [31]	pubmed.ncbi.nlm.nih.gov/14006056/ 0.1% 1 matches
<input checked="" type="checkbox"/> [32]	pubmed.ncbi.nlm.nih.gov/27536698/ 0.1% 1 matches
<input checked="" type="checkbox"/> [33]	chemrxiv.org/engage/chemrxiv/article-details/60c7588ebb8c1af8033dca4a#:~:text=The present manuscript describes the,radical reported up to date. 0.1% 1 matches
<input checked="" type="checkbox"/> [34]	www.ncbi.nlm.nih.gov/pmc/articles/PMC5536142/ 0.1% 1 matches
<input checked="" type="checkbox"/> [35]	journals.plos.org/plosone/article/file?id=10.1371/journal.pone.0118555&type=manuscript 0.1% 1 matches
<input checked="" type="checkbox"/> [36]	www.vedantu.com/biology/cell-organelles#:~:text=Cell organelles/structures can be,endoplasmic peroxisome, and the cytoskeleton. 0.1% 1 matches
<input checked="" type="checkbox"/> [37]	www.sciencedirect.com/science/article/abs/pii/0003269774903789 0.1% 1 matches
<input checked="" type="checkbox"/> [38]	www.ncbi.nlm.nih.gov/pmc/articles/PMC3466135/ 0.1% 1 matches
<input checked="" type="checkbox"/> [39]	www.sciencedirect.com/science/article/abs/pii/S004040201930345X 0.1% 1 matches
<input checked="" type="checkbox"/> [40]	www.ncbi.nlm.nih.gov/pmc/articles/PMC8912752/ 0.0% 1 matches
<input checked="" type="checkbox"/> [41]	www.ncbi.nlm.nih.gov/pmc/articles/PMC9901003/ 0.1% 1 matches
<input checked="" type="checkbox"/> [42]	www.sciencedirect.com/science/article/abs/pii/S0146638097000582 0.0% 1 matches
<input checked="" type="checkbox"/> [43]	pubmed.ncbi.nlm.nih.gov/20837440/ 0.1% 1 matches

15 pages, 4419 words

 The document contains a suspicious mixture of alphabets. This could be an attempt of cheating.

PlagLevel: 11.0% selected / 24.9% overall

128 matches from 44 sources, of which 43 are online sources.

Settings

Data policy: *Compare with web sources, Check against my documents*

Sensitivity: *High*

Bibliography: *Bibliography excluded*

Citation detection: *Highlighting only*

Whitelist: --

Cytotoxicity and apoptosis induction of zinc ferrite (ZnFe₂O₄) nanoparticle through the Oxidative Stress Pathway in Human Breast cancer cells

Abstract: The nanoparticles of Zinc Iron oxide have been broadly used in various fields such as solar cells, photo catalysis, hydrogen storage, sensors etc. ^[10] Here, the zinc iron oxide nanoparticles (ZnFe₂O₄NPs) was prepared via solution process and characterized in detail with instruments such as X-ray diffraction pattern (XRD), field emission scanning electron microscopy (FESEM), transmission electron microscopy (TEM), Fourier transform infrared spectroscopy and thermogravimetric analysis (TGA). ^[10] The characterization studies revealed that the average individual size of each NP is ~27±1 nm size. The FTIR shows the functional band of metal and oxygen was obtained at 570 cm⁻¹. Although, the processing and use of zinc iron oxide based nanostructures are very widely utilized in industries but a limited studies are available towards the cancer studies. The current work explores the application of ZnFe₂O₄NPs against breast cancer cells (MCF-7) to examine the cytotoxicity, oxidative stress and morphological variations using 3-(4,5-dimethylthiazol-2-yl)-2,5-diphenyltetrazoliumbromide (MTT), neutral red uptake (NRU), lipid peroxidation (LPO), reduced glutathione (GSH), assays after 24 h of treatment. Dose dependent drop in cell survival was seen in MTT and NRU assays. A significant increase in LPO, was observed in MCF-7 cells exposed to ZnFe₂O₄NPs after 24 h of treatment. However, the GSH levels in MCF-7 cells exposed to ZnFe₂O₄NPs decreased significantly after 24 h. Further, the study of apoptotic gene expression was seen by real time PCR analysis was also conducted and described.

Keywords: MCF-7 cells; ^[3] Zinc ferrite nanoparticles; Cytotoxicity; Oxidative stress.

[3] ▶ 1. Introduction

Due to the exponential growth of nanotechnology in recent decades and its wide range of applications, nanomaterials (NMs) are already found in everyday products such as paints, building materials, cosmetics and in the food industry, exerting a great impact on today's society [1,2,3].^{[18]▶} The large surface area:^{[12]▶} volume ratio results in an increase in the reactivity of nanoparticles (NPs). Importantly, this affects the mechanisms of interaction with biological systems and these are far from being completely elucidated due to their complexity [4]. Even NPs of the same material can show different toxicities due to a small differences in the size, shape, degree of aggregation, coating or surface charge etc [5]. In addition, as soon as the NPs come into contact with the biological environment, the adsorption of biomolecules and the formation of the so-called "protein corona" begins, modifying the properties of NPs and making their behaviour difficult to predict [6].^{[32]▶} Finally, the degree of toxicity varies depending on the dose of NPs used and the exposure time [7].

Magnetic iron oxide NPs constitute one of the promising systems in the field of biomedicine. Their low toxicity, biocompatibility, excellent magnetic properties (super para magnetism) and easy and versatile surface functionalization, open a wide range of possible biomedical applications. These applications cover the diagnostic functions as contrast agents in magnetic resonance imaging [8], biosensors [9] or cellular labelling [10], as well as therapeutic functions, such as magnetic hyperthermia [11], controlled drug release [12], tissue regeneration [13] or gene therapy [14].^{[17]▶} Recent advances in nanomedicine have led to the development of intelligent NMs, combining both diagnosis and therapeutic functions, providing synergistic effects known as "theragnostics" [15].

NMs are tiny materials with dimensions ranged between 1 to 100 nm, having electronic, optical and mechanical properties [16] NMs have high impact on many fields of sciences including physics, engineering, biology, agriculture and food sciences due to its unique physico chemical

properties [17]. NMs are broadly classified into three categories namely NPs, nanoclays and nanoemulsions [18]. Having this technology, multiple advantages to the delivery of natural compounds in the treatment of cancer and other human diseases. In particular, NPs were used to increase the delivery of nutrients into the cells [19].

^[11] Zinc ferrite ($ZnFe_2O_4$) has the same properties as homogeneous catalysts and is also easily extracted from the reaction by an external magnet and does not require more rigorous methods such as filtration or centrifugation. In comparison to homogeneous catalysts, heterogeneous ones have been exclusively studied because of their easy recovery and separation from the reaction mixture [20]. The use of magnetically separable catalysts is a well-favored and fascinating strategy to bridge the split between heterogeneous and homogeneous catalysis processes [21]. As a main member of the ferrite family, $ZnFe_2O_4$ has promising potential for use as novel catalytic support. Additionally, the surface hydroxyl groups over them facilitate their surface modifications with a wide variety of organic compounds.

There are few reports on Fe_3O_4 toxicity especially under in vivo conditions and moreover some researchers showed controversial results. For instance, some studies have reported minimal toxicity in some concentrations and some others have shown non-toxicity effects under in vivo conditions [22]. Others have reported damages and changes in liver, kidney, gastrointestinal and neuronal systems in vivo [23, 24].

^[13] Ferrites are important nanomagnetic materials in the chemical industry due to their unique characteristics and potential uses, including magnetic resonance imaging, treatment of cancer, and biomedical drug delivery ^[40] [25, 26, 27]. Meanwhile, the relatively high magnetic properties of zinc modified ferrite (Zn ferrite) NPs have intensively attracted the researchers' attention in all areas of biomedicine and bio-engineering, such as contrast-enhanced magnetic resonance imaging, cell separation, hyper-thermia, detoxification of biological fluids, drug delivery, and tissue regeneration [28, 29,30]. These MNPs enjoy high magnetization values and sizes smaller

than 100 nm and thus have similar chemical and physical properties. It is also necessary that the surfaces of particles have been coated with nontoxic materials and also be biocompatible [31, 32]. Using zinc ferrite NPs in pharmaceuticals necessitate a comprehensive study of the plausible toxicity. In the previous studies, some useful applications have been reported such as induction of chromosomal aberration in the sunflower root meristematic cells [33], the production of genotoxicity and cytotoxicity in human amnion epithelial cell lines (WISH) [34] oxidative stress in different human cells [35], and cytotoxicity and antioxidant activity [36]. The experimental inconsistencies observed in methods, materials, and used cell lines, however, make it difficult to achieve acceptable conclusions.^{[21]▶} In addition, nanotoxicological assessments should be considered as a physicochemically comprehensive characterization of the materials.^{[21]▶} along with their lower toxicity [37].

^{[3]▶} Zinc ferrite NPs also exhibit low toxicity in place of other metallic cations.^{[3]▶} Hence, it can be easily substantiated that zinc ion incorporation should be a better option to improve novel non-lanthanide-based MRI contrast agents.^{[3]▶} In recent years, because of the fabrication of NPs, innumerable studies have been concentrated to research and enhance its properties [38].^{[3]▶} Zinc Ferrite exposes superparamagnetic behaviour among other ferrites [39].^{[3]▶} Zinc ferrite has been extensively employed in different commercial applications such as absorbent materials, photocatalysts, gas sensors, catalysts [40],^{[3]▶} magnetic resonance imaging (MRI), and Li ion batteries due to its significant magnetic and electrical properties.^{[3]▶} Recently, Nano ferrites have been widely examined because they exhibit magnificent physical and chemical properties compete with bulk counterparts [39].^{[3]▶} Between structure, composition, and properties of NPs, zinc ferrite set a marvellous example of direct relation.^{[3]▶} When prepared as a bulk material, the zinc-iron oxide has a spinel structure AB_2O_4 with a tetrahedral A site occupied by Zn^{2+} ions and an octahedral B site by Fe^{3+} ions.^{[3]▶} Based on the distribution of cations, spinels can be either

normal like zinc spinel or inverse with half of the trivalent ions in the tetrahedral position and the other half together with the divalent ions in the octahedral sites [41].

^[3]▶ The present manuscript describes the synthesis of zinc ferrite nanoparticles via solution process and characterized in detail. The grown particles were well utilized against the breast cancer cells (MCF-7), which is widely a common disease in world wide. ^[3]▶ A number of biological studies such as MTT, NRU assays, ROS, GSH, LPO and RT-PCR were conducted. Including to these a possible discussion was also described in detail.

^[5]▶ 2. Materials and methods

2.1. Experimental

The synthesis of zinc ferrite was performed with the use of zinc nitrate hexahydrate, iron nitrate nonahydrate and sodium hydroxide. The chemicals related to the formation of nanoparticles were purchased from Aldrich chemical corporation, U.S.A ^[9]▶ and used as received. In an experiment, the zinc nitrate hexahydrate (0.1M), and iron nitrate nonahydrate (0.3M) were prepared in double distilled water in a 250 ml capacity beaker, under constant stirring. Once the solution was dissolute completely, sodium hydroxide (0.03M) was added to this mixture dropwise and stirred completely. The pH of the prepared mixture was noted which reached to 12.75 and then after transferred to the relaxed it for 6 hours (h) at 90°C. The obtained precipitates were filtered and washed with distilled water/ethanol. ^[16]▶ The product dried at room temperature for 48 h and keep for further analysis.

2.2. Characterizations of the prepared product

The X-ray powder diffractometer (XRD, Cu_{Kα} radiation ($\lambda = 1.54178 \text{ \AA}$) ^[6]▶ with rotation angle ranging from 10° to 80° with 6°/min scanning speed, was used for the analysis of the prepared powder. ^[10]▶ Morphology of the prepared powder was analysed with using field emission scanning electron microscopy (FESEM) as described earlier [42][ref]. Also the Fourier transform

infrared (FTIR) spectroscopy was analysed in the range of 400–4000 cm^{-1} . The thermal stability test was performed with terms of thermal gravimetric analysis (TGA) instrument (Mettler Toledo AG, Analytical CH-8603, Schwerzenbach, Switzerland) was also conducted for the analysis of prepared product. For this experiment ~6.8 mg of powder was loaded into alumina crucibles (Al_2O_3) and heated till to 800°C with a heating ramp of 20°C/min under nitrogen gas with a flow of 20 mL/min.

2.3. Cell culture

Human liver cancer (HepG2) cells (ATCC, US) were maintained in DMEM culture medium supplemented with 10% fetal bovine serum (FBS), 100 U/mL penicillin as an antibiotic, and 100 $\mu\text{g}/\text{mL}$ streptomycin at 37 °C in a humidified 5% CO_2 incubator.

2.4. ^[5] Cell viability assays (MTT and NRU)

The cell viability was determined MTT (3-(4,5-dimethylthiazol-2-yl)-2,5-diphenyltetrazolium bromide) assay and carried out as according to the previously described [43] protocol with some minor modifications. Cells were seeded in 96-well plates ($\sim 1 \times 10^4$ cells/ well, 200 $\mu\text{L}/\text{well}$). The cells plates were kept in an incubator at 37°C with humid environment for to grow the cells until 70-80% confluency. The sample (Zn-Fe NPs) which contains culture medium was removed after 24h and washed three to four times with PBS. Thereafter, the MTT solution in medium (final MTT concentration 10 $\mu\text{g}/\text{mL}$) was added and incubated the cells at 37°C for 2h. Once the incubation time was completed, the MTT solution was removed without disturbing the cells and DMSO (200 $\mu\text{L}/\text{well}$) was added, the plates were shaken gently for to dissolve the formazan crystals in the wells. The plate absorbance was observed with microplate reader (Multiskan Ex, Thermo Scientific, China) at 550 nm. The (%) cells viability was calculated as described below formula. The values represent mean \pm SD of 3 independent replicas of the experiment.

$$\% \text{viability} = [(\text{total cells} - \text{viable cells}) / \text{total cells}] \times 100$$

Including the MTT, ZnFe₂O₄NPs induced lysosomal fragility, as an indicator of cytotoxicity, was quantitated by NRU assay following a previously described method [44,45].^{[7]▶} For the NRU assay, cells were seeded in 96-well plates and allowed to grow overnight at 37°C in a CO₂ incubator (5% CO₂ humidity). Once the incubation was completed, the media was discarded and fresh medium (RPMI-1640) was refilled.^{[4]▶} The cells were allowed to grow further for 48 h at 37 °C in a CO₂ incubator (5%, 95% humidity).^{[7]▶} After 48h, the cell culture medium was discarded and washed with PBS.^{[7]▶} The neutral red (NR) dye (50 µg/mL) freshly prepared in culture medium was added in all wells, thereafter, cells were incubated with NR dye for 3 h at 37°C in a CO₂ incubator (5%, humidity 95%).^{[7]▶} Then, NR dye was discarded, and cells were washed again with PBS to completely remove the dye.^{[6]▶} Finally, the absorbance of red color developed in the wells was measured at 550 nm on a microplate reader.

2.5. Detection of intracellular ROS

The reactive oxygen species (ROS) produced in the cells were measured with using 2, 7-dichloro di hydrofluoresce in diacetate (DCFH-DA; Sigma Aldrich, USA) dye, which is utilized as a fluorescent agent and followed the protocol as described earlier [46]. The DCFH-DA inertly enters the cell and it reacts with ROS to form the highly fluorescent compound dichlorofluorescein (DCF). The cells were exposed with the processed material for 24 h, and washed well with PBS and incubated for 30 min in DCFH-DA (20 µM) in dark medium at 37°C. Once the reaction of DCFH-DA with control and treated cells were completed, it was analysed with intra- cellular fluorescence using fluorescence microscope.

2.6. Mitochondrial membrane potentials

The MMP were determined with MCF-7 cells in control and treated samples determined by JC-1 (5, 50, 6, 60-Tetrachloro-1, 10, 3, 30-tetraethyl benzimidazolylcarbocyanine iodide). In healthy cells with high mitochondrial membrane potential, JC-1 forms complexes known as J-

aggregates with intense fluorescence [47].^[30] On the other hand, in apoptotic cells with lower membrane potential, JC-1 remains in the monomeric. The cells were seeded at appropriate densities in plate reader. After the treatment, media was aspirated and labelled with 5 μ M JC-1 in HEPES buffered HBSS for 20 min. Fluorescence of JC-1 aggregate (red in color) and JC-1 monomer (green in color) in cells were taken by a fluorescence microscope (Leica DMI8, using objective 20 \times and LAS core software) using green filter cube.

2.7. Glutathione level

For Glutathione (GSH) level measurement, MCF-7 cells was cultured in 25 cm² flasks. The cells were exposed to 50, 100, and 200 μ g/mL of Zn-FeNPs for 24 h. Subsequently, the cells were lysed in cell lysis buffer [^[5]1 \times 20 mM Tris-HCl (pH 7.5)^[5], 150 mM NaCl, 2.5 mM sodium pyrophosphate, 1 mM Na₂EDTA, and 1% Triton]. Centrifuge 15,000 \times g for 10 min at 4 $^{\circ}$ C, then supernatant, obtained was kept on ice until following [48].^[16] Briefly, a mixture of 0.1 mL^[37] of cell extract (supernatant) and 0.9 mL of 5% TCA was centrifuged (2300 \times g for 15 min at 4 $^{\circ}$ C). Thereafter, 0.5 mL^[34] of supernatant was added to 1.5 mL of 0.01% 5, 5-dithio-bis-(2-nitrobenzoic acid) (DTNB) and measured spectrophotometrically at 412 nm.

2.8. Lipid peroxidation (LPO)

Lipid peroxidation (LPO) was assayed by the following of [49]. MCF-7 cells were exposed to 50, 100, and 200 μ g/mL of Zn-Fe NPs for 24 h. Briefly, 0.1 mL of cell extract and 1.9 mL^[12] of 0.1 M^[4] sodium phosphate buffer (pH 7.4)^[5] were incubated at 37 $^{\circ}$ C for 1 h.^[6] After incubation, cells were precipitated with 5% TCA and then centrifuged to 2300 \times g for 15 min, to collect the supernatant. After incubation, 1.0 mL^[5] of 1% TBA was added to the supernatant and put in hot water for 15 min. After cooling, the absorbance was taken at 532 nm.

2.9. Real-time PCR (RT-PCR)

Total RNA was purified from MCF-7 cells from untreated and treated with ZnFe₂O₄NPs for 24 h using the RNeasy mini Kit (Qiagen). As the manufacturing protocol RNA was isolated there purity were determined by Nanodrop 8000 spectrophotometer (Thermo Scientific, USA). The integrity of RNA was confirmed by visualized on 2% agarose gel with the documentation system (Universal Hood II, BioRad, USA). The cDNA was prepared by the MLV reverse transcriptase (GE Health Care, UK) For the quantification of apoptotic of apoptotic and anti-apoptotic gene was determined by using Roche[®]LightCycler[®]480 (96-well block), following the cycling program. Reaction mixture of 20 µl taking 75 ng of the cDNA and 5 µM of each primer with 2 × of SYBR Green I dye Roche Diagnostics. The cycling conditions at 95 °C for 10 min denaturation step, followed by 40 cycles of 95 °C for 15 s denaturation, 60 °C for 20 s annealing, and 72 °C for 20s elongation steps [50]. Data were normalized by GAPDH, a house keeping control gene. All the experiment was done in triplicate.

2.10. Data analysis

The statistical analysis data. Statistical significance was measured at p 0.05.^[24] The experiments were carried out in triplicates manner. The images were captured at constant exposure time.

3. Results

3.1. Size and morphological results (XRD, FESEM and TEM results)

The crystallographic structure of ZnFe₂O₃ nanoparticles was recognised of powder XRD assessment. The powder XRD patterns is presented in Fig.1. The peak positions are 29.98 (220), 35.28 (311), 36.92 (222), 42.84 (400), 53.2 (422), 56.64 (511) and 62.22 (440). All appears diffraction peaks were indexed to the face centered regular spinel cubic structure (JCPDS card No. 89-1009) [51]. No other impurity peaks were detected, which endorse the purity of the NPs. The strong sharp peaks suggested that ZnFe₂O₄NPs were well crystallized.^[23] The average crystallite size of ZnFe₂O₄NPs was estimated using Scherrer's equation.^[19] The calculated average crystallite size was ~27±1nm.

Morphology of ZnFe₂O₄NPs was further examined by FESEM and TEM. Figure 2A and B display the typical FESEM and TEM micrographs of ZnFe₂O₄NPs, respectively. The micrograph indicate that ZnFe₂O₄NPs have spherical morphology with average particle size of around 27±1 nm.

3.2. Chemical functional analysis (FTIR results)

The functional groups in the prepared powder was examined and assigned the FTIR spectroscopy and represent as Fig.3. The peak at 570 cm⁻¹ is related to ZnFe₂O₄ whereas the bands at 3200-3600 cm⁻¹ correspond to H-O-H mode of vibration.^[9] The small asymmetric stretching mode of vibration of O-H was observed between 1627 cm⁻¹.^[9] The symmetric and asymmetric stretching vibrational peak occurs between 1383 cm⁻¹ which designates the vibration of NO₃⁻¹ ions [52, 53]^[3](Vijayakumar et al., 2016; Kumar et al., 2017).

3.3. Thermogravimetric analysis (TGA results)

Thermogravimetric analysis (TGA) provides the information related to the % mass loss with increasing the temperature. Fig.4. shows two-step weight loss for the prepared sample, the first one is related to the used solvent elimination whereas other one is the stabilization phase respectively. From the obtained data reveals that the initial step phase starts at 311°C and completed at 430°C with a weight loss of 1.60%. The secondary weight loss starts at 530°C, which is also knows as chemical decomposition phase, completed at 900°C with a total weight loss was 3.10%. The secondary phase shows the stabilization of the prepared material and from with this information it shows that a very minute quantity was loosed. From the experiment it reveals that the prepared material is highly stable at high temperature and are in consistent with other studies (XRD and FTIR).

3.4. Microscopic results for cells morphology

The morphology of the grown/cultured cells and treated cells ($\text{ZnFe}_2\text{O}_4\text{NPs}$) were examined via microscopic study at 24 h incubation periods in a range of different concentrations of $\text{ZnFe}_2\text{O}_4\text{NPs}$ (50, 100 and 200 $\mu\text{g}/\text{mL}$) (Fig.5).^[35] The initially grown cells was used as a control (Fig.5) to compare the treated cells. The treated cells morphologies were captured and displayed as Fig.5. The image shows that the long and oval shaped structure with nucleated positions initially but once the incubation time increases, the cells size were further increased. Fig. 5B, At initial treated sample at low concentration (50 $\mu\text{g}/\text{mL}$) of cells sizes were decreased and higher concentration (100 to 200 $\mu\text{g}/\text{mL}$) of $\text{ZnFe}_2\text{O}_4\text{NPs}$, the growth of cells was much affected, which are very clear from the obtained images (Fig.5C and D). From this experiment, it concluded that at higher concentration of NPs 100 to 200 $\mu\text{g}/\text{mL}$, cells were damage completely (Fig.5).

3.5. MTT assay

The toxicity in cells was very widely observed via MTT assay as detailed described above with the incorporation of $\text{ZnFe}_2\text{O}_4\text{NPs}$. The obtained data reveals that the viability of cancer cells were diminished with the incorporation of $\text{ZnFe}_2\text{O}_4\text{NPs}$ and these data's were concentration/dose-dependent. The cancer cells viability was decreases at 24 h 100%, 101%, 100%, 93%, 86%, 67% and 55% (Fig.6) for the concentrations of 2, 5, 10, 25, 50, 100 and 200 $\mu\text{g}/\text{mL}$ respectively (p 0.05 for each). The MTT calculation shows that at initial concentrations (2, 5, 10 $\mu\text{g}/\text{mL}$) of material doesn't shows any change in the cells viability, whereas at higher concentration of $\text{ZnFe}_2\text{O}_4\text{NPs}$ shows a sequential change in the viability of cells and cytotoxicity was much influenced.

3.6. NRU assay

Including the MTT assay, the cytotoxicity was again observed via NRU assay in present of $\text{ZnFe}_2\text{O}_4\text{NPs}$. The NRU assay was calculated as described in the material and method with

using control and treated cancer cells, exposed in a range of different concentrations from 2-200 µg/ml for 24 h incubation. The experiment shows that viability of cells were affected with the incorporation of ZnFe₂O₄NPs and affected the cells growth. The NRU assay was decreases at 24 h 107%, 107%, 102%, 97%, 88%, 71% and 53% (Fig.7) for the concentrations of 2, 5, 10, 25, 50, 100 and 200 µg/mL correspondingly (p 0.05 for each). As MTT assay, the NRU data's also in consistent and express that the cells viability initially not affected much whereas as the concentrations of ZnFe₂O₄NPs exceeded the cytotoxicity was much influenced.

3.7. ROS generation in breast cancer cells (MCF-7) with ZnFe₂O₄NPs

A sequential change in ROS data was observed in breast cancer cells (MCF-7) after the exposure of ZnFe₂O₄NPs at 50, 100 and 200 µg/mL concentrations for 24 h (Fig. 8) with control. From the observed ROS with captured image and presented as Fig. 8A) and bar graph (Fig. 8B) shows that the ROS is increases with the increase of ZnFe₂O₄NPs concentrations as compared to control cells. The ROS were increase at 50 µg/mL, 100 µg/mL and 200 µg/mL were 120, 141, 171% as compared to control (100%) (Fig.8B).

3.8. Mitochondrial Membrane Potential (MMP) with ZnFe₂O₄NPs

The MMP induction was observed with JC-1 red, JC-1 green and channel merged imaging and of monomer/aggregate both IC₅₀ and control MCF-7 cells treated with ZnFe₂O₄NPs (Fig. 9A). The level of MMP with control was determined at different concentration of ZnFe₂O₄NPs in MCF-7 cells exposed to 24 h at 25, 50, 100 and 200µg/ml are 89%, 75%, 49% and 43% as shown in Fig.9B. The decrease in MMP level was recorded in terms of fluorescence intensity of mitochondrial-specific dye JC-1. It is clearly presented that ZnFe₂O₄NPs decreased the fluorescence intensity.

3.9. Glutathione level

Depletion in GSH level in cultured MCF-7 cells exposed to 25, 50, 100, 200 $\mu\text{g}/\text{mL}$ concentrations of $\text{ZnFe}_2\text{O}_4\text{NPs}$ for 24 h are summarized in Fig. 10A. The result indicates that rotenone decreased the GSH levels in a dose-dependent manner. Fig. 10A. Shows a significant decrease in the GSH activity at higher concentrations as compared to the untreated control. A concentration-dependent significant decrease of 90%, 82%, 73% and 62% were observed in GSH activity at 25, 50, 100, and 200 $\mu\text{g}/\text{mL}$ of $\text{ZnFe}_2\text{O}_4\text{NPs}$, respectively as compared to untreated control (Fig. 10A).

3.10. Lipid peroxidation

The $\text{ZnFe}_2\text{O}_4\text{NPs}$ -induced LPO in MCF-7 cells are summarized in Fig10B. A concentration-dependent significant increase in LPO was observed. An increase of 112, 124, 135 and 153% at 25, 50, 100, and 200 $\mu\text{g}/\text{mL}$ respectively were found in MCF-7 cells exposed for 24 h with control.

3.11. RT-PCR

The quantitative RT-PCR study was performed to check the mRNA level in MCF-7 cancer cells treated with $\text{ZnFe}_2\text{O}_4\text{NPs}$ for 24 h at a concentration of 100 $\mu\text{g}/\text{ml}$. A number of marker genes were selected such as genes (p53, bax, casp3 and bcl2) of the evaluation of mRNA level in cancer cells. The data shows a change with marker genes and upregulation of apoptotic genes in MCF-7 cells ($p < 0.05$ for each gene). The mRNA levels of tumor suppressor of p53 gene (fold change-2.6), the pro-apoptotic gene bax (fold change-1.6) and casp-3 (fold change-3.8) were upregulated with $\text{ZnFe}_2\text{O}_4\text{NPs}$, whereas expression of bcl-2 (fold change-0.7), which is an anti-apoptotic gene, was down regulated in cells treated with $\text{ZnFe}_2\text{O}_4\text{NPs}$ (Fig.11).

4. Discussion

The basic study of the prepared material ($\text{ZnFe}_2\text{O}_4\text{NPs}$), the objective of the present study is to evaluate the biological efficiency against breast cancer (MCF-7) cells in terms of cytotoxic response. A long range of concentrations (2, 5, 10, 25, 50, 100 and 200 $\mu\text{g}/\text{mL}$) of the material

was opted and interacted with the cancer cells for 24 h. The MTT, NRU data shows that the viability of the cells were much dependent upon utilized doses/concentration of the material and are corroborated with published literature [54]. From the observation, it reveals that the cells cytotoxicity were depended with factors such as cells activity, the morphology of the nano or microstructure, media concentrations etc.^[8] are responsible for the cell death [55].^[15] The reactive oxygen species (ROS) also played a key role in cytotoxicity assessment.^[15] It's believed that NPs or any foreign substance when reacted with cells in media, have possibility to produce reactive oxygen species (ROS) and are responsible the toxicological change in cells [56]. The change with ROS also responsible in the imbalance in cells organelles structures such DNA, protein, and lipids and affected their mechanism. The cells were much influenced also their functions were affected and lead to cell death [57]. The detailed study presented here, express that the ZnFe₂O₄NPs are responsible to produce ROS at specified doses in MCF-7 cells and that why the cell cytotoxicity may occurred [58]. With the obtained data's such as XRD, FESEM, TEM, FTIR, TGA and toxicological study with MTT, NRU assays, ROS, RT-PCR and others related (MMP and LPO) data's, it may postulates that the toxicity in cells are dependent with ZnFe₂O₄ NPs in a dose dependent manner.

^[3] 5. Conclusions

The summary of current work shows that the zinc ferrite nanoparticles (ZnFe₂O₄NPs) were formed with solution method and characterized in detail. The X-ray diffraction pattern reveals the estimated size (27±1nm), crystallinity, phases of product. The morphological analysis such as FESEM and TEM are in very well consistent with the XRD data and shows the average size of each NPs are ~28nm, spherical in shape.^[3] The FTIR express that band at ~570 cm⁻¹ represents the formation of ZnFe₂O₄NPs without any other impurity.^[3] The cells morphology was studied via inverted microscopy and it reveals that different concentrations of ZnFe₂O₄ NPs express a sequential cytological effect on of on cancer cells.^[3] The MTT and NRU assays were measured

the viability of cells and the results clearly showed that at initial doses ZnFe₂O₄NPs not to provide any information in change in the cells growth, whereas when the doses were increased the viability of the cells were highly influenced. The ROS generation analysis also in consistent with the MTT and NRUs data and shows the ZnFe₂O₄NPs are effective against breast cancer cells. Also the gene expression study with marker genes (P53, caspase-3, Bax, Bcl2) reveals that apoptosis happens in breast cancer cells with ZnFe₂O₄NPs.